Observations of Aircraft Dissipation Trails from GOES

DAVID P. DUDA

Center for Atmospheric Sciences, Hampton University, Hampton, Virginia

PATRICK MINNIS

Atmospheric Sciences, NASA Langley Research Center, Hampton, Virginia

(Manuscript received 4 January 2001, in final form 13 July 2001)

ABSTRACT

Two cases of aircraft dissipation trails (distrails) with associated fall streak clouds were analyzed with multispectral geostationary satellite data. One dissipation trail was observed in a single cloud layer on 23 July 2000 over southeastern Virginia and the Chesapeake Bay. Another set of trails developed at the top of multilayer cloudiness off the coasts of Georgia and South Carolina on 6 January 2000. The distrails on both days formed in optically thin, midlevel stratified clouds with cloud-top heights between 7.6 and 9.1 km. The distrail features remained intact and easily visible from satellite images over a period of 1–2 h despite winds near 50 kt at cloud level. The width of the distrails became as large as 20 km within a period of 90 min or less. Differences between the optical properties of the fall streak particles inside the distrails and those of the clouds surrounding the trails allowed for the easy identification of the fall streak clouds in either the 3.9-μm brightness temperature imagery, or the 10.7-μm minus 12.0-μm brightness temperature difference imagery. Two independent remote sensing retrievals of both distrail cases showed that the fall streaks had larger particle sizes than the clouds outside of the trails, although the three-channel infrared retrieval was better at retrieving cloud properties in the multilayer cloud case.

1. Introduction

One of the most commonly observed effects of jet aircraft on the atmosphere is the formation of condensation trails (contrails) due to the mixing of moist jet engine exhaust with cool ambient air. However, under some atmospheric conditions, an opposite effect can occur and an aircraft dissipation trail (distrail) can be formed.

Unlike contrails, published reports of distrails observed from space are rare (Corfidi and Brandli 1986). Dissipation trails often remain unnoticed even from the ground as they are less well known to the public than contrails, and often appear only briefly within an otherwise unremarkable cloudy sky. Since many distrails probably escape casual observation, the frequency of distrail formation is hard to estimate, but it may be more than negligible. As part of some contrail research, one of the authors completed a manual survey of daily 4-km-resolution geostationary satellite imagery over the course of one year. Although no conscious effort was made to look for distrails, five possible cases of distrail formation were observed during the 1-yr period.

Although they are relatively rare, dissipation trails can form in several ways. Jet engine exhaust is not only moist, but also hot, and this heat tends to dry the atmosphere. If the ratio of added heat to added moisture is large enough, an aircraft flying through a cirriform cloud can evaporate the cloud in its path (Appleman 1953). Aircraft motion can also produce short-lived distrails by the turbulent mixing of dry air just above a thin cloud layer (Scorer 1972). Finally, aircraft flying through supercooled clouds can initiate glaciation of the cloud (and the production of ice crystals) along its path, and the resulting ice particles grow rapidly and fall out, leaving a distrail (Scorer 1972; Rangno and Hobbs 1983; Sassen 1991).

Contrails have long been of interest to atmospheric scientists as they are believed to have a radiative effect on climate similar to cirrus (Fu and Liou 1993), and are expected to grow in frequency as air traffic increases. Although distrail frequency is much less than contrail frequency, any changes in the microphysical properties of the clouds affected by distrails are of interest scientifically as they would represent a possible effect on the atmosphere by aviation. This study attempts for the first time to assess these changes from space.

Corresponding author address: Dr. David P. Duda, NASA Langley Research Center, Mail Stop 420, 21 Langley Boulevard, Hampton, VA 23681-2199.
E-mail: d.p.duda@larc.nasa.gov

Two case studies of dissipation trails that were detected in satellite imagery from the *Geostationary Operational Environmental Satellite-8* (*GOES-8*) will be presented. The first study examines a distrail that formed on 23 July 2000 over southeastern Virginia and drifted over the Chesapeake Bay. The second case involves a set of dissipation trails that appeared on 6 January 2000 in clouds off the coast of South Carolina and Georgia. Since these trails appear to have formed in the top layer of two-layer cloudiness, they are a challenging case study for the satellite remote sensing of cloud properties. This paper describes the development of the distrails in both case studies and presents the first satellite remote sensing retrievals of cloud properties in and near the wake of distrails.

2. Observations

Figure 1 shows a time series of enhanced channel 1 (0.65 μm) visible reflectance ($R_{0.65}$) images of a distrail observed over southeastern Virginia on 23 July 2000 between 2225 and 2302 UTC. As the dissipation trail formed around 2232 UTC, a fall streak cloud in the center of the distrail also developed, which was observed later by one of the authors from the ground (Fig. 2). The fall streak cloud was produced from glaciated particles in the center of the dissipation path.

A visible image of the distrail at 2310 UTC is shown in Fig. 3. The distrail and the associated fall streak have both grown in size (to 16 and 4 km wide, respectively) and advected over the Chesapeake Bay. From the Wallops Island (WAL) sounding at 0000 UTC 24 July 2000 and the rate of distrail advection [245° at 43 kt (22.1 m s^{-1})], the height of the cloud containing the distrail was estimated to be between 7.7 and 9.6 km. The WAL sounding shows a moist layer between 8.5 and 9.1 km, suggesting the cloud-top height was near 9 km. We note that another distrail appears in Fig. 3 directly east of Wallops Island.

On 6 January 2000, several distrails developed off the coasts of South Carolina and Georgia over a period of several hours. Figure 4 presents two distrails observed at 1815 UTC. The difference between the channel 4 (10.7 μm) infrared brightness temperature ($T_{10.7}$) and the channel 5 (12.0 μm) split-window brightness temperature ($T_{12.0}$) was used to enhance the contrast between the distrails and the surrounding cloud. The distrails tended to lower the brightness temperature difference between these channels as the fall streak particles in the center of the distrail are larger than the particles in the surrounding cloud layer [see Minnis et al. (1998) for plots of $T_{10.7} - T_{12.0}$ as a function of particle size]. Figure 5 shows the corresponding visible image at 1815 UTC. As in Figs. 1 and 3, both the distrails and their associated fall streak clouds are visible in Fig. 5. The width of the western distrail inside the box in Fig. 5 is roughly 8 km. By 1945 UTC, the width of the distrail increased to 20 km (Fig. 6). Corfidi and Brandli (1986) reported distrails exceeding 28 km in width, and like the distrails reported here, remained remarkably intact despite high winds at cloud level. An examination of Figs. 5 and 6 show that the distrail was advected at a speed of 53 kt (27.3 m s^{-1}) between 1815 and 1945 UTC. Comparing the distrail speed and direction (260°) with the Charleston, South Carolina (CHS), soundings at 1200 and 0000 UTC on 7 January 2000, the cloud level where the distrail formed was around 7.6 km. This height is confirmed by the 0000 UTC sounding at CHS which contains a moist layer between 415 and 387 hPa (7.2–7.7 km).

We note that in the 0000 UTC sounding the air above the upper-tropospheric moist layer becomes extremely dry. The dewpoint depression between 387 and 381 hPa (7.7–7.8 km) increases from 5 to 34 K. The dry air above the cloud layer may help in the production of the dissipation trails. Similar distrails produced by other aircraft also appear in the GOES imagery until at least 2245 UTC.

3. Remote sensing analysis

Two remote sensing schemes were used to infer cloud parameters in and around the dissipation trails. The first method was the visible–infrared–solar infrared technique (VIST; Minnis et al. 1995). The VIST uses an iterative technique to simultaneously determine effective particle size [for ice clouds, an effective diameter, D_e, is derived, while for water clouds an effective radius, R_e, is retrieved (Hansen and Travis 1974; Han et al. 1994); for consistency, all R_e retrievals have been converted to D_e in this paper], visible optical depth (τ), cloud-top temperature (T_c), and cloud-top height (z_c) given the observed visible reflectance, the channel 2 (3.9 μm) solar infrared brightness temperature ($T_{3.9}$), the channel 4 brightness temperature and estimates of the clear-sky visible reflectance, and the clear-sky channel 2 and 4 brightness temperatures. The method computes temperatures and reflectances for a range of particle sizes and optical depths for the given solar zenith, viewing zenith, and relative azimuth angles using the cloud emittance and reflectance parameterizations of Minnis et al. (1998) and a visible channel surface–atmosphere–cloud reflectance parameterization (Minnis et al. 1995). The cloud parameters follow from the best match between the observed and modeled brightness temperatures and reflectances.

The VIST retrieval algorithm has been compared to passive and active radiometric measurements at surface sites, primarily at the Atmospheric Radiation Measurement (ARM) southern Great Plains (SGP) central facility in Oklahoma (Dong et al. 1997; Mace et al. 1998; Garreaud et al. 2001). Cloud property retrievals using the Visible Infrared Scanner (VIRS) on the Tropical Rainfall Measuring Mission (TRMM) satellite show good agreement with the ground-based measurements. The average difference between the VIST cloud-top

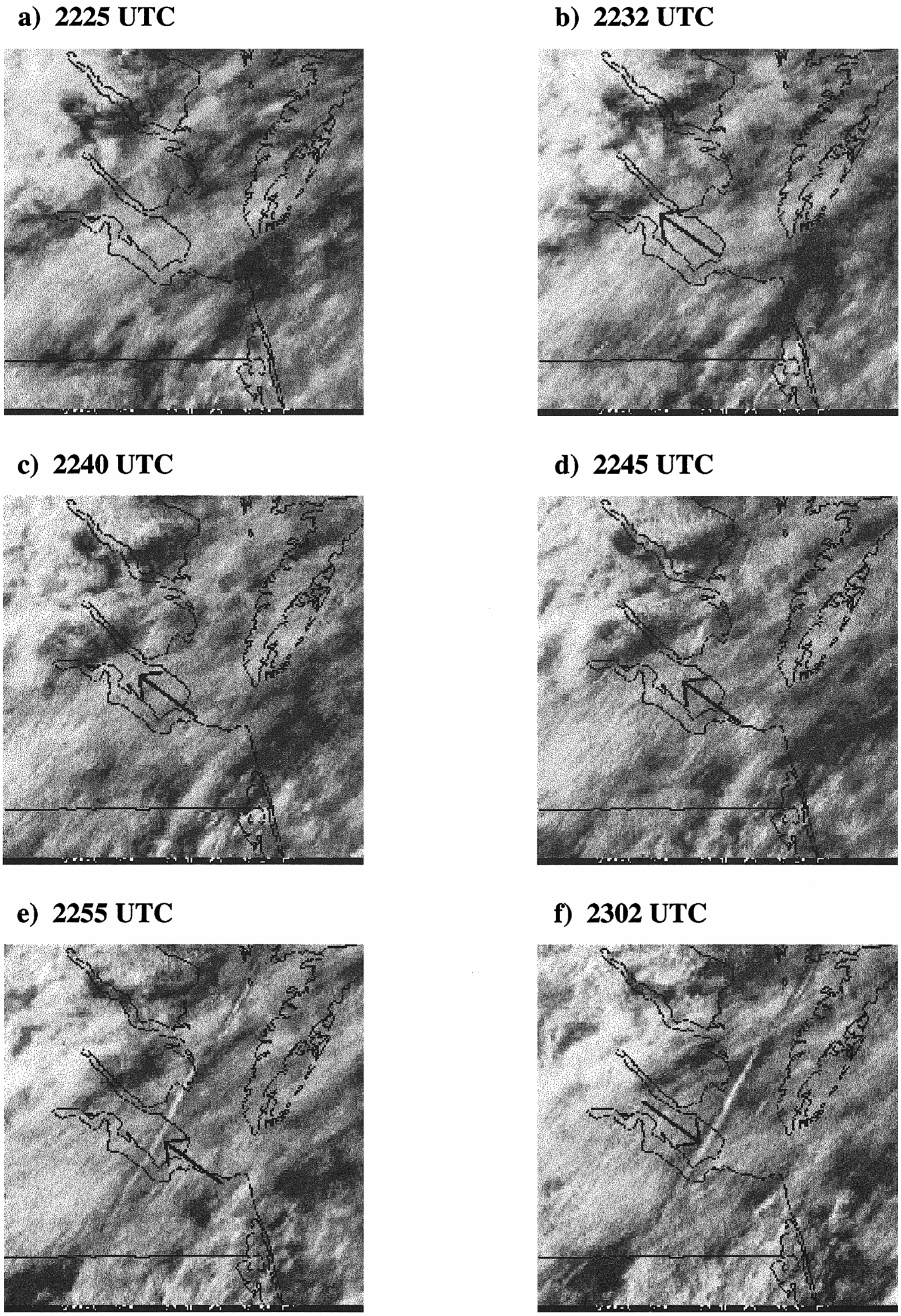

FIG. 1. Time series of dissipation trail and associated fall streak cloud development from enhanced *GOES-8* channel 1 visible reflectance ($R_{0.65}$) imagery on 23 Jul 2000 between 2225 and 2302 UTC. The black arrows indicate the location of the distrail and fall streak.

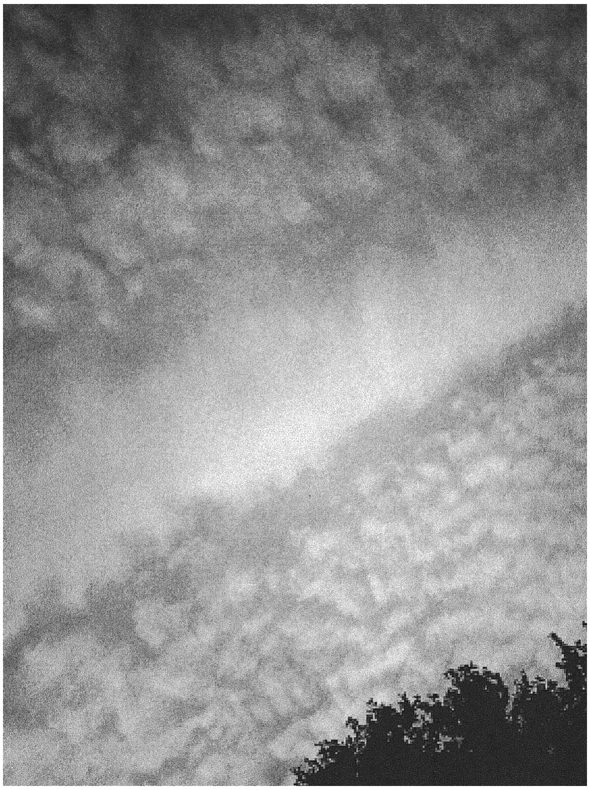

FIG. 2. Dissipation trail and fall streak cloud observed from the ground at approximately 2245 UTC 23 Jul 2000.

height estimates and the ARM-derived results were -0.4 km for thick clouds and -1.1 km for thin cirrus clouds (i.e., the VIST estimates lower cloud heights) with a standard deviation around 1.8 km. The mean difference between the satellite and ground-based retrievals of optical depth in single-layered stratus was 1.1 km, while the mean particle diameter differences were 1.2 μm with a standard deviation of 3.6 μm.

VIST retrievals using GOES and Advanced Very High Resolution Radiometer (AVHRR) data have also been compared to in situ aircraft measurements of a wave cloud containing small ice crystals during the spring 1996 Subsonic Clouds and Contrails Effects Special Study campaign (SUCCESS; Young et al. 1998). The mean particle diameters, retrieved from AVHRR data collocated with the aircraft flight track in a wave cloud over Colorado, were 18.7 μm compared to 15.5 μm and 11.8 μm from two independent cloud particle measurements in the aircraft. The mean particle size retrieved from the wave cloud region by GOES data collected approximately 10 min after the aircraft data was 17.9 μm, and is consistent with the AVHRR retrieval.

The second method was the solar infrared–infrared–split window technique (SIST; Minnis et al. 1995). Like the VIST, the SIST is an iterative technique that uses multichannel brightness temperatures to compute cloud parameters. For a given optically thin cloud ($\tau < 6$) and the background (clear sky or cloudy) temperatures for channels 2, 4, and 5, the $T_{3.9}$ minus $T_{10.7}$ difference, the $T_{10.7}$ minus $T_{12.0}$ difference, and $T_{10.7}$ are modeled for a range of T_c, D_e (or R_e depending on cloud phase), and τ. The cloud parameters for both channels 2 and 5 follow from the best matches between the observed and modeled values of the three brightness temperature quantities. The phase of the cloud is selected based on T_c. If the mean value of T_c from the two channels is greater than 273 K, only the water-droplet models are used. If the mean value of T_c is less than 233 K, only the ice-crystal models are considered. Otherwise, the phase is selected by comparing how closely the channel 2 and 5 cloud parameters agree with each other (the phase resulting in the smaller overall difference is chosen). The final values of D_e, T_c, and τ are determined by averaging the channel 2 and 5 results for the selected phase.

An advantage of the SIST is that it can produce relatively accurate values of T_c. Smith et al. (1997) compared SIST-derived cloud-top heights of optically thin clouds with those measured by lidar at the ARM SGP facility. The mean and standard deviation of the SIST minus lidar-derived heights were 0.1 and 1.2 km, respectively.

For both satellite-retrieval methods, estimates of clear-sky reflectances and brightness temperatures are necessary. These values were obtained from clear-sky pixels within or near the analysis region. A separate analysis routine, the layer bispectral threshold method (LBTM) of Minnis et al. (1993), is used to identify clear-sky pixels in the analysis area.

4. Results

a. 23 July 2000—Southeastern Virginia and Chesapeake Bay

The black box in Fig. 3 shows the area where the VIST analysis was performed in the 23 July case. An inspection of the 23 July 2000 GOES imagery time series and the WAL sounding at 0000 UTC on 24 July 2000 determined that the analysis region contained single-layer cloudiness. (In addition, the author observed no clouds below the deck containing the distrail).

The results of the VIST analysis for the 23 July case are shown in Table 1. For this analysis, an arbitrary $T_{10.7}$ minus $T_{3.9}$ difference (i.e., channel 4 minus channel 2) threshold was used to determine which pixels in the analysis region were inside and outside the distrail path. A plot of the $T_{10.7} - T_{3.9}$ showed a bimodal peak separated by a minimum at 20 K. The bimodal peak occurred since the distrails tended to suppress the measured brightness temperature difference for two reasons. First, the mean optical depth of the cloudiness in the path of the distrail (0.94, derived from SIST) is less than the optical depth (1.45, derived from SIST) outside of

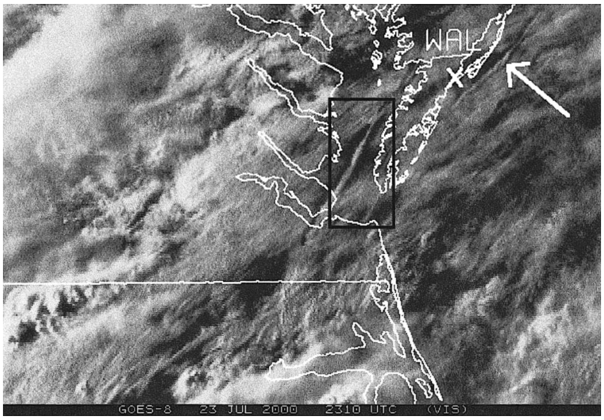

FIG. 3. Dissipation trail and associated fall streak cloud from enhanced *GOES-8* $R_{0.65}$ imagery at 2310 UTC 23 Jul 2000. The white × shows the location of Wallops Island, VA (WAL) sounding, and the black rectangle is the area of VIST analysis on the distrail fall streak. The white arrow indicates the location of another distrail that is visible in the image.

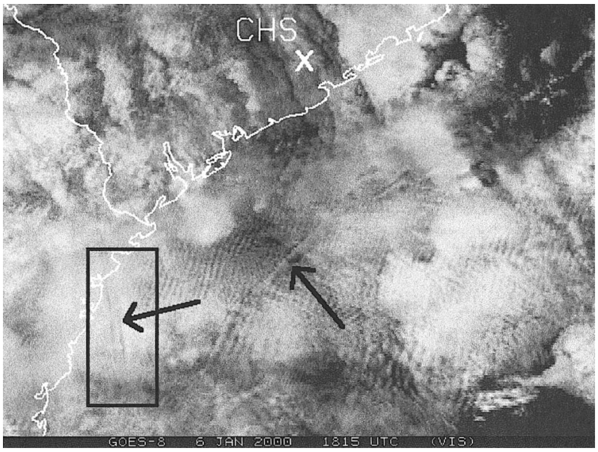

FIG. 5. Same as Fig. 4 but from enhanced *GOES-8* $R_{0.65}$ imagery; resolution 1 km. Black arrows indicate two distrail paths with fall streak clouds. The black rectangle is the area of VIST analysis on the western distrail/fall streak.

the path. Second, the large, icy fall streak particles reflect less solar radiation at 3.9 μm than the smaller supercooled water droplets in the undisturbed cloud. Thus, pixels with a $T_{10.7} - T_{3.9}$ of less than 20 K were considered to be in the path of the distrail, while those greater than 20 K were outside of the distrail.

The retrievals for the 23 July case were made using the 0000 UTC Wallops Island sounding on 24 July 2000. The mean particle diameter of the fall streak particles in the distrail region was estimated to be 17.8 μm, while the mean diameter of the particles in the cloud surrounding the trail was 12.6 μm.

The VIST analysis objectively determines the phase of the cloud particles using a series of threshold tests based on several factors including cloud temperature and estimates of the reflection of solar radiation in the 3.9-μm channel. VIST determined that nearly all of the pixels in the analysis box were liquid water. However, fall streak clouds are most likely supercooled particles that freeze during the turbulent passage of an aircraft through the cloud layer (Scorer 1972; Rangno and Hobbs 1983). This conclusion is also supported by the observation that frozen particles would grow faster by diffusion than the surrounding liquid water clouds. When the VIST analysis was modified to assume ice particles (hexagonal columns) in the distrail path and liquid water particles outside the distrail, the mean retrieved size (i.e., diameter) of the fall streak particles inside the distrail increased to 30.7 μm and the mean diameter of the cloud droplets decreased to 9.8 μm (Table 1).

Because of the large solar zenith angle in the 23 July case (78°), some VIST-derived cloud properties are dif-

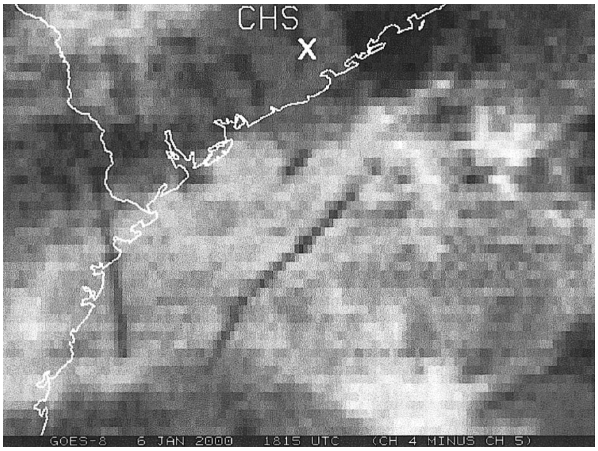

FIG. 4. Two distrails from *GOES-8* $T_{10.7} - T_{12.0}$ brightness temperature imagery at 1815 UTC 6 Jan 2000; resolution is expanded to 1 km. The white × shows the location of the Charleston, SC (CHS) sounding.

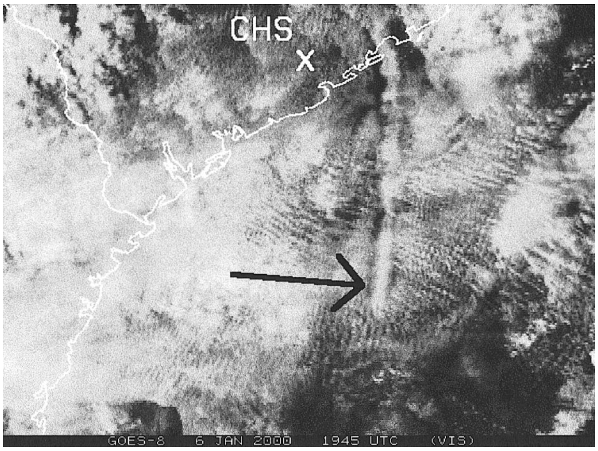

FIG. 6. Same as Fig. 5 but for 1945 UTC. The black arrow indicates the location of the western distrail and fall streak also visible in Figs. 4 and 5.

TABLE 1. VIST-derived cloud properties from 2310 UTC 23 Jul 2000.

Data	D_e (μm)	$\sigma(D_e)$ (μm)	T_{cloud} (K)	z_{cloud} (km)
Inside distrail (objective analysis)	17.8	10.2	267.0	5.29
Outside distrail (objective analysis)	12.6	14.6	255.8	7.26
Inside (assume ice)	30.7	16.3	243.0	9.06
Outside (assume water)	9.8	4.4	256.3	7.20

ferent than those inferred from other observations. The cloud-top height estimated from the Wallops Island rawinsonde sounding (around 9 km) was much higher than the VIST-retrieved cloud-top height (7.2 km), but the rawinsonde-derived height compares well with the height of the fall streak cloud that is retrieved when ice particles are assumed. In addition, the VIST retrieval of the optical depth (not shown in Table 1, but is approximately 15) is too large when compared to the visual appearance of the cloud in Fig. 2. These discrepancies are probably caused by the high sensitivity of VIST at large solar zenith angles.

To derive a more accurate retrieval of the cloud–fall streak properties, the SIST was used on the 23 July 2000 case. Because the SIST is based on emitted radiation, it cannot be used under all conditions. The SIST works better for single-layer cloud systems, and can only retrieve τ and D_e for optically thin clouds. The model must also be run with the proper boundary conditions to account for the effects of the solar radiation at 3.9 μm.

To minimize the effects of reflected solar radiation, the clearest area in the analysis box determined from a LTBM analysis were used to obtain the $T_{3.9}$, $T_{10.7}$, and $T_{12.0}$ values that were used as background conditions in the SIST analysis. The large $T_{10.7} - T_{12.0}$ value (5.5 K) in this area demonstrates that none of the analysis region was completely cloud-free, but suggests that a low-level haze or subpixel-scale cloudiness was present over the Chesapeake Bay during the time of the retrieval. The SIST results are presented in Table 2. The mean retrieved optical depth of both the fall streak (0.94) and the cloud surrounding the distrail (1.45) are much more consistent with the appearance of the cloud in Fig. 2 than the VIST results (both were around 15). The mean SIST-derived cloud particle diameter in the fall streak (61.6 μm) was twice as large as the VIST retrieval mean, while the diameter of the water droplets in the surrounding cloud averaged 26 μm. Even SIST determined a cloud-top height different from that inferred from the WAL sounding. The mean height of the cloud top outside of the distrail path was 10.4 km while the mean height of the fall streak was 8.2 km. It is likely that the SIST cloud-top height retrieval is still affected by solar radiation since the SIST cannot account for horizontal inhomogeneity in the solar component of the background radiance field at 3.9 μm.

b. 6 January 2000—South Carolina and Georgia coasts

The VIST analysis for the 6 January 2000 case is indicated by the black box in Fig. 5. An inspection of the GOES imagery time series and the presence of two separate moist layers in the 0000 UTC 7 January 2000 CHS sounding indicated that the distrail formed in the top layer of a two-layer cloud system. As shown later, the presence of the lower cloud layer has a strong impact on the ability of the remote sensing retrieval to accurately determine cloud properties.

The properties of the cloud layer below the distrail were found by analyzing the layer with the VIST (between 1315 and 1545 UTC) before the layer containing the dissipation trail drifted over it. The height of the low cloud was estimated from the early-day VIST analysis to be near 2.0 km, and the cloud particle diameters ranged from 16 to 20 μm. This retrieval is confirmed by the 1200 UTC 6 January 2000 and 0000 UTC 7 January 2000 Charleston soundings, which both show a moist boundary layer capped by a 4–6 K inversion. The top of the moist layer increases in elevation from 1.7 km at 1200 UTC to 2.5 km at 0000 UTC on 7 January. A higher cloud drifted over the area after 1700 UTC, and by 1815 UTC two long distrails formed in the cloud layer. A retrieval of the cloud properties in and around the western distrail in Fig. 5 at 1815 UTC is shown in Table 3. In the VIST objective analysis, all pixels both inside and outside the distrail path were retrieved as liquid water. The mean particle diameter inside the dissipation trail was 30.0 μm, while the mean diameter in the cloud outside the trail was 16.4 μm. When the VIST analysis was modified to assume ice particles in the distrail path, the mean retrieved diameter of the fall streak particles was only 17.7 μm, nearly the same size as the liquid water cloud droplets outside of the trail.

A $T_{10.7} - T_{3.9}$ threshold was also used in this case to determine which pixels in the analysis region were inside and outside the distrail path. For this analysis box, a brightness temperature difference threshold of 26.0 K was used, since brightness temperature differences larg-

TABLE 2. SIST-derived cloud properties from 2310 UTC 23 Jul 2000. The particle sizes for water pixels are in parentheses.

Data	D_e (μm)	$\sigma(D_e)$ (μm)	Optical depth	T_{cloud} (K)	z_{cloud} (km)
Inside distrail	61.6	52.9	0.94	249.0	8.20
Outside distrail	53.2 (26.0)	50.6 (15.8)	1.45	233.2	10.38

TABLE 3. VIST-derived cloud properties from 1815 UTC 6 Jan 2000.

Data	D_e (μm)	$\sigma(D_e)$ (μm)	Optical depth	T_{cloud} (K)	z_{cloud} (km)
Inside distrail (objective analysis)	30.0	6.6	15.1	262.2	5.34
Outside distrail (objective analysis)	16.4	2.4	15.0	259.7	5.68
Inside (assume ice)	17.7	2.6	9.2	261.2	5.48

er than 26.0 K included pixels outside of the linear path of the distrail. [The $T_{10.7} - T_{12.0}$ value could also be used to find the distrail path, since the larger fall streak particles in the center of the distrail lower the bright temperature difference between these bands (Parol et al. 1991). A $T_{10.7} - T_{12.0}$ threshold of 3.5 K produced a similar discrimination between distrail and nondistrail pixels as the $T_{10.7} - T_{3.9}$ threshold].

The retrieved cloud-top height of the cloud outside of the distrail area was near 5.7 km, about 2 km lower than the cloud-top height (7.6 km) estimated from the speed and direction of the distrail drift and the location of moisture in the CHS sounding. If the cloud level were at 7.6 km, then the cloud temperature would be approximately 246 K based on the Charleston soundings. Highly supercooled droplets have been observed in altocumulus with temperatures as cool as 243 K (Heymsfield et al. 1991). Since at least two levels of cloud are apparent in the retrieval area, the VIST cloud-top height is probably an underestimate as the top layer is not optically thick enough to prevent the lower cloud from affecting the retrieval. The optical depth retrievals are also affected by multilayer cloudiness and include contributions from both layers of clouds.

The presence of a lower cloud appears to affect all retrieved cloud properties (including optical depth, cloud temperature, cloud-top height and particle size) in the 6 January 2000 case. Thus, the SIST analysis was also run on this case to verify the VIST results.

Despite the complications of the multilayer cloud system on 6 January 2000, a reliable retrieval may be possible for this case using SIST. Since the distrail formed in a thin cloud and the lower cloud layer is relatively uniform, an accurate retrieval should be possible by treating the lower cloud layer as the background (and the cloud layer containing the distrail as the ''only'' cloud layer).

A $T_{3.9}$ image of the distrails at 1815 UTC is shown in Figure 7. The distrails are readily visible in the image since the larger, icy fall streak particles reflect less solar radiation at 3.9 μm than the smaller supercooled water droplets in the surrounding cloud. The black box in the figure indicates the area of the SIST analysis on 6 January 2000, which is the same as the VIST analysis region in Fig. 5.

A SIST analysis of the low cloud in the analysis region showed that it was optically thick ($\tau > 10$) with a cloud-top height near 1 km. Using the $T_{3.9,}$ $T_{10.7}$, and $T_{12.0}$ brightness temperatures of the low cloud as the background, a second SIST analysis of the higher cloud containing the distrail was made. The analysis showed that the optical depth of the higher cloud was much smaller than the value computed from the VIST. The mean retrieved optical depth of the cloud in the region outside of the distrail was 2.2. The retrieved optical depths of the fall streaks in the dissipation trail were smallest in the center of the distrail region, and the mean value was 1.6.

Unlike the VIST, the SIST analysis indicated that most (86%) of the particles in the higher cloud were ice. The lower-layer cloud reflectances weight the overall reflectances resulting in an interpretation of a water cloud by VIST. In the SIST analysis, the lower-layer contribution is relegated to the background radiance; its effect on the optical depth and phase retrieval is minimized. Despite the differences in phase and optical depth, the particle sizes retrieved from both techniques were similar. In the cloud outside of the distrail, the mean retrieved cloud particle diameter of the ice particles was 11.1 μm; the mean diameter of the water droplets was 13.5 μm. The mean particle diameter of the ice particles inside of the distrail was 24.4 μm, although the particle sizes in the center of the trail were as large as 67 μm. The average retrieved cloud temperature outside of the dissipation trail was 241 K, corresponding to a mean cloud-top height of 8.4 km. The cloud-top heights estimated from SIST appear to be more consistent with those derived earlier from the rawinsonde measurements than do the VIST results. The retrieved mean values inside the distrail were 247.5 K and 7.35 km respectively.

Since the distrail analyzed in this retrieval was starting to become visible in the 1745 UTC imagery, the particles appear to be no more than 45 min old. This

TABLE 4. SIST-derived cloud properties from 1815 UTC 6 Jan 2000. The particle sizes for water pixels are in parentheses.

Data	D_e (μm)	$\sigma(D_e)$ (μm)	Optical depth	T_{cloud} (K)	z_{cloud} (km)
Inside distrail	24.4	10.0	1.6	247.5	7.35
Outside distrail	11.1 (13.5)	4.2 (3.0)	2.2	241.3	8.42

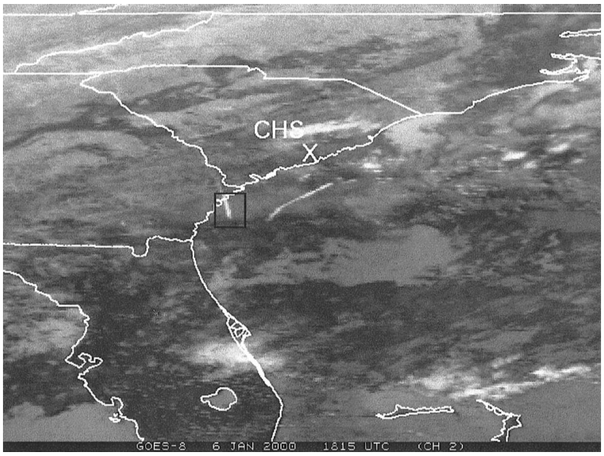

FIG. 7. Two distrails from enhanced *GOES-8* channel 2 (3.9 μm) brightness temperature ($T_{3.9}$) imagery at 1815 UTC 6 Jan 2000. The black rectangle is the area of SIST analysis on the western distrail/fall streak region.

result suggests a sedimentation rate of the fall streak particles of at least 0.4 m s^{-1} in the distrail. Estimates of columnar ice crystal fall speeds based on observations (Heymsfield and Iaquinta 2000) suggest that ice crystals at least 320 μm in diameter are needed to have such large fall speeds. Errors in the estimation of the fall streak particle sizes may account for part of this discrepancy, as well as errors in the fall streak cloud-top height retrieval due to the coarse resolution of the satellite. As mentioned earlier, the width of the distrail at the time of the SIST retrieval was only 8 km, and the width of the fall streak cloud is roughly half as large. Thus, the fall streak cloud has a width of only one satellite pixel at 1815 UTC.

5. Summary

Two cases of distrails observed in *GOES-8* multispectral data were presented. In the first example from 23 July 2000, a distrail formed in a single cloud layer over southeastern Virginia and the Chesapeake Bay. The second example showed distrails that developed on 6 January 2000 at the top of a multilayer cloud system off the coast of South Carolina and Georgia. Remote sensing analyses of both cases were made using the VIST and the SIST techniques of Minnis et al. (1995). The satellite observations and analyses showed the following results:

- The distrails on both days formed in optically thin, midlevel stratified clouds. The cloud-top height (temperature) estimated from nearby rawinsonde observations was 9.1 km (242 K) in the 23 July 2000 case, and 7.6 km (245 K) in the 6 January 2000 case. A dry layer that may have enhanced the production of distrails also capped the 6 January 2000 cloud. The microphysical properties derived by satellite also suggest that cloud layers that form distrails and fall streak clouds might often be composed of relatively small droplets.
- In both cases, the distrail features remained intact and easily visible from the satellite images over a period of one or two hours despite high winds (near 50 kt) at cloud level. The width of the fall streak clouds and the distrail appeared to grow over time in both cases. The 23 July 2000 distrail expanded in width from 1 to 16 km in 40 min, while the 6 January 2000 distrail expanded in width from 8 to 20 km over a period of 90 min.
- The cloud property retrievals were complicated by a large solar zenith angle in the 23 July 2000 case and multilayer cloudiness on the 6 January 2000 case. For both cases, the SIST results appear to be more reliable as the SIST computed more accurate cloud heights compared with height estimates derived from nearby rawinsonde observations. The 6 January 2000 case study suggests that the SIST may be successfully used for cloud property retrievals in thin cirriform clouds over optically thick low-level clouds.
- The microphysical properties of the fall streak clouds resulting from the formation of the distrail were different from those in the surrounding cloud layer. Both the VIST and the SIST computed fall streak particle diameters larger than the diameters of the liquid water droplets outside of the distrail. For the VIST, the inside distrail (outside distrail) liquid water particle sizes were 30.7 μm (9.8 μm) on 23 July 2000, and 17.7 μm (16.4 μm) on 6 January 2000; while for the SIST, the diameters were 61.6 μm (26.0 μm) on 23 July 2000, and 24.4 μm (13.5 μm) on 6 January 2000. The cloud optical depth of the fall streak cloud within the distrail path was less than that determined from the surrounding cloud layer. The mean SIST-derived fall streak optical depths were about 70% as large as the optical depths in the surrounding cloud layer.
- Differences in the optical properties of the cloud particles inside and outside of the dissipation trails allowed for their easy identification in either the channel 2 (solar infrared; 3.9 μm) or the channel 4 minus channel 5 (infrared minus split-window; 10.7 μm $-$ 12.0 μm) imagery.

These case studies [and the distrail described by Corfidi and Brandli (1986)] demonstrate that aircraft occasionally produce dissipation trails in midlevel clouds with widths on the order of 10 to 20 km, and lengths of over 100 km. Both cases were identifiable in geostationary satellite data due to the creation of a glaciated fall streak cloud with microphysical properties sufficiently different from the surrounding undisturbed cloud deck to create a visible signature in the 3.9- μm channel satellite data. This property of the distrails is useful in identifying such features from space, and could be used in future studies to determine whether dissipation trails occur frequently enough to produce any quantifiable effect on the radiative budget of the atmosphere.

Acknowledgments. The authors wish to thank David Young and Bill Smith, Jr. for the interactive cloud analysis software. This research was supported by the NASA Atmospheric Effects of Aviation Program, NASA Grant NAG-1-2135, and the Environmental Sciences Division of the U.S. Department of Energy Interagency Agreement DE-AI02-97ER62341 as part of the Atmospheric Radiation Measurement Program.

REFERENCES

Appleman, H., 1953: The formation of exhaust condensation trails by jet aircraft. *Bull. Amer. Meteor. Soc.,* **34,** 14–20.

Corfidi, S., and H. W. Brandli, 1986: GOES views aircraft distrails. *Natl. Wea. Dig.,* **11,** 37–39.

Dong, X., T. P. Ackerman, E. E. Clothiaux, P. Pilewskie, and Y. Han, 1997: Microphysical and radiative properties of boundary layer stratiform clouds deduced from ground-based measurements. *J. Geophys. Res.,* **102** (D20), 23 829–23 843.

Fu, Q., and K.-N. Liou, 1993: Parameterization of the radiative properties of cirrus clouds. *J. Atmos. Sci.,* **50,** 2008–2025.

Garreaud, R., J. Rutllant, J. Quintana, J. Carrasco, and P. Minnis, 2001: CIMAR-5: A snapshot of the lower troposphere over the subtropical southeast Pacific. *Bull. Amer. Meteor. Soc.,* **82,** 2193–2207.

Han, Q., W. B. Rossow, and A. A. Lacis, 1994: Near-global survey of effective droplet radii in liquid water clouds using ISCCP data. *J. Climate,* **7,** 465–497.

Hansen, J. E., and L. D. Travis, 1974: Light scattering in planetary atmospheres. *Space Sci. Rev.,* **16,** 527–610.

Heymsfield, A. J., and J. Iaquinta, 2000: Cirrus crystal terminal velocities. *J. Atmos. Sci.,* **57,** 916–938.

——, L. M. Miloshevich, A. Slingo, K. Sassen, and D. O'C. Starr, 1991: An observational and theoretical study of highly supercooled altocumulus. *J. Atmos. Sci.,* **48,** 923–945.

Mace, G. G., T. P. Ackerman, P. Minnis, and D. F. Young, 1998: Cirrus layer microphysical properties derived from surface-based millimeter radar and infrared interferometer data. *J. Geophys. Res.,* **103** (D18), 23 207–23 216.

Minnis, P., P. W. Heck, and D. F. Young, 1993: Inference of cirrus cloud properties from satellite-observed visible and infrared radiances. Part II: Verification of theoretical radiative properties. *J. Atmos. Sci.,* **50,** 1305–1322.

——, and Coauthors, 1995: Cloud optical property retrieval (subsystem 4.3). Cloud analyses and radiance inversions (subsystem 4), Vol. III, Clouds and the Earth's Radiant Energy System (CERES) algorithm theoretical basis document, NASA Ref. Publ. 1376, Vol. 3, 135–176.

——, D. P. Garber, D. F. Young, R. F. Arduini, and Y. Takano, 1998: Parameterizations of reflectance and effective emittance for satellite remote sensing of cloud properties. *J. Atmos. Sci.,* **55,** 3313–3339.

Parol, F., J. C. Buriez, G. Brogniez, and Y. Fouquart, 1991: Information content of AVHRR channels 4 and 5 with respect to the effective radius of cirrus cloud particles. *J. Appl. Meteor.,* **30,** 973–984.

Rangno, A. L., and P. V. Hobbs, 1983: Production of ice particles in cloud due to aircraft penetrations. *J. Climate Appl. Meteor.,* **22,** 214–232.

Sassen, K., 1991: Aircraft-produced ice particles in a highly supercooled altocumulus cloud. *J. Appl. Meteor.,* **30,** 765–775.

Scorer, R. S., 1972: *Clouds of the World: A Complete Colour Encyclopedia.* David & Charles, 176 pp.

Smith, W. L., Jr., L. Nguyen, D. P. Garber, D. F. Young, P. Minnis, and J. Spinhirne, 1997: Comparisons of cloud heights derived from satellite and ARM surface lidar data. *Proc. 6th ARM Science Team Meeting,* San Antonio, TX, U.S. Department of Energy, 287–291.

Young, D. F., P. Minnis, D. Baumgardner, and H. Gerber, 1998: Comparison of in situ and satellite-derived cloud properties during SUCCESS. *Geophys. Res. Lett.,* **25,** 1125–1128.